Parameter identification for improved performance of model-based control of hydraulic manipulators

Lionel Hulttinen, Janne Koivumäki, and Jouni Mattila

Abstract—In addition to hydraulic manipulators' complex and nonlinear dynamics, their dynamic behaviour typically also involve significant parameter uncertainties. This study aims to evaluate the performance of nonlinear model-based control of hydraulic manipulators, by comparing (*i*) a controller using model parameters acquired from manufacturer datasheets and computer-aided modeling tools, in relation to (*ii*) a controller exploiting parameter identification methods to estimate the model parameters from pressure transmitter and joint encoder data collected from the plant. Experimental results show that the proposed control scheme relying on the identified parameters results in significant improvement of Cartesian position tracking performance in free-space motion, in comparison to using the nominal parameters.

I. INTRODUCTION

Hydraulic manipulators are imposed with complex and nonlinear dynamic behaviour, which renders their control design a challenging task. Nonlinear model-based (NMB) control methods have been shown to provide a viable solution to address these system nonlinearities [1]. The main idea behind NMB control is to utilize inverse plant models in order to calculate necessary feedforward actions that can help reducing the control burden of feedback loops. In the context of hydraulic manipulators, this translates into proactively generating required actuator forces (and control valve outputs) from desired motion dynamics, based on the dynamic models of the hydraulic actuators and the mechanical structure of the manipulator.

However, accurate plant models are tedious to acquire, since the nonlinear plant models used in NMB control laws are subject to parameter uncertainty (e.g., nominal valve flow coefficients stated by manufacturer datasheets do not reflect reality). Computer-aided design (CAD) software are commonly used to acquire sophisticated guesses about the manipulator inertial parameters. However, CAD modeling is prone to errors due to the uncertainty related to material densities, and detailed modeling of minor elements (such as hosing and integrated valve packages) is time-consuming. Moreover, actuator friction has a significant effect on the force output of hydraulic cylinders, yet friction parameters cannot be acquired by CAD modeling. Therefore, it would be beneficial to identify the model parameters from data collected from the plant instead, in order to avoid manual adjustment of friction parameters and flow coefficients by trial-and-error.

What comes to hydraulic manipulators, research has been almost entirely focused on parameter identification [2–4],

Lionel Hulttinen, Janne Koivumäki, and Jouni Mattila are with the Department of Automation Technology and Mechanical Engineering, Tampere University, Finland. Emails: `firstname.surname@tuni.fi`

without much emphasis on identification for model-based control. In [5], a NMB controller was developed based on Lagrangian dynamics, and all model parameters involved in the control laws were identified from experimental data. The main focus in [5] was in providing a stability-guaranteed control design and identifying model parameters for eased controller deployment, but no comparisons were made between the control performance when using the identified parameters versus the nominal parameters.

In the present study, in contrast to [5], we use the recursive Newton-Euler (N-E) dynamics as the basis of our control design and parameter identification. In addition, in order to verify the feasibility of the identified inertial parameters, the system is modeled using CAD software (see Fig. 1) to provide reference values. Special emphasis is paid for evaluating the control performance between the nominal parameter control and identified parameter control.

The rest of the paper is structured as follows. Section II provides the mathematical background to model the system behaviour. In Section III, inertial and frictional parameters of a hydraulic manipulator are identified from measured cylinder chamber pressures and joint encoder angles, assuming a priori knowledge of the geometric dimensions. In Section IV, a NMB control strategy (inspired by the N-E dynamics -based virtual decomposition control [6], and the state-of-the-art results achieved in [7–10] for hydraulic manipulators) exploiting the identified parameters is described. Finally, experiments carried on the physical plant are presented in Section V, which demonstrate the effectiveness of the proposed controller, and reveal significant improvements in relation to the results presented in [5].
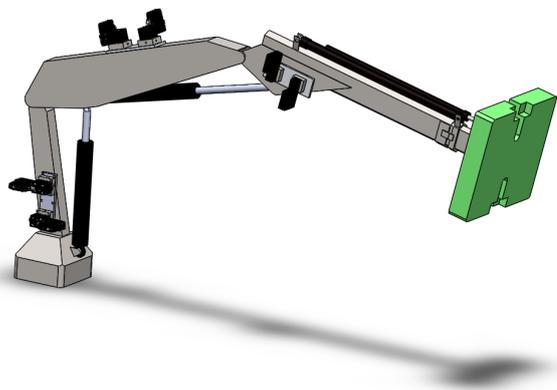

Fig. 1. CAD model of the studied manipulator.

II. MATHEMATICAL PRELIMINARIES

A. Rigid-body dynamics

This paper exploits Featherstone's spatial vector algebra [11] to represent the rigid-body dynamics. The spatial velocity vector of the ith boxy-fixed coordinate frame is defined as

$$\mathbf{v}_i = \begin{bmatrix} \boldsymbol{\omega}_i \\ \boldsymbol{v}_i \end{bmatrix} \tag{1}$$

where $\boldsymbol{\omega}_i = [\, \omega_{xi} \; \omega_{yi} \; \omega_{zi} \,]^{\mathrm{T}}$ is the angular velocity vector and $\boldsymbol{v}_i = [\, v_{ix} \; v_{iy} \; v_{iz} \,]^{\mathrm{T}}$ is the linear velocity vector measured in the ith body-fixed coordinate frame. The spatial force/torque vector measured in the ith body-fixed coordinate frame is defined as

$$\mathbf{f}_i = \begin{bmatrix} \boldsymbol{\tau}_i \\ \boldsymbol{f}_i \end{bmatrix} \tag{2}$$

where $\boldsymbol{\tau}_i = [\, \tau_{ix} \; \tau_{iy} \; \tau_{iz} \,]^{\mathrm{T}}$ is the torque vector and $\boldsymbol{f}_i = [\, f_{xi} \; f_{yi} \; f_{zi} \,]^{\mathrm{T}}$ the force vector measured in the ith body-fixed coordinate frame. Spatial forces and velocities can be transformed between two consecutive frames $\{i\}$ and $\{i+1\}$ using kinematic wrench transmission matrices $^{i+1}_i\mathbf{X}$ as follows

$$\mathbf{v}_{i+1} = {}^{i+1}_i\mathbf{X}\, \mathbf{v}_i \tag{3}$$

$$\mathbf{f}_i = {}^{i+1}_i\mathbf{X}^{\mathrm{T}}\, \mathbf{f}_{i+1} \tag{4}$$

In the boxy-fixed formulation of the recursive N-E algorithm [11, 12], forward propagation of velocities and accelerations is carried according to the following recursive formulas

$$\mathbf{v}_{i+1} = {}^{i+1}_i\mathbf{X}\, \mathbf{v}_i + \mathbf{s}_i \dot{q}_i \tag{5}$$

$$\dot{\mathbf{v}}_{i+1} = {}^{i+1}_i\mathbf{X}\, \dot{\mathbf{v}}_i + \mathbf{s}_i \ddot{q}_i + \begin{bmatrix} [\boldsymbol{\omega}_{i+1}\times] & 0 \\ [\boldsymbol{v}_{i+1}\times] & [\boldsymbol{\omega}_{i+1}\times] \end{bmatrix} \mathbf{s}_i \dot{q}_i \tag{6}$$

where $\dot{q}_i$ is joint velocity, $\ddot{q}_i$ joint acceleration, $\mathbf{s}_i$ is a unit rotation vector, e.g., for a revolute joint $\mathbf{s}_i = [\, 0 \; 0 \; 1 \; 0 \; 0 \; 0 \,]^{\mathrm{T}}$, and $[(\cdot)\times]$ is the cross product operator, defined as

$$[\boldsymbol{\omega}_i \times] = \begin{bmatrix} 0 & -\omega_{zi} & \omega_{yi} \\ \omega_{zi} & 0 & -\omega_{xi} \\ -\omega_{yi} & \omega_{xi} & 0 \end{bmatrix}$$

The spatial velocity of the fixed base frame $\{0\}$ equals to $\mathbf{v}_0 = \mathbf{0}$. To account for gravity, the base frame is ficticiously accelerated against the direction of gravitational acceleration by defining $\dot{\mathbf{v}}_0 = [\, 0 \; 0 \; 0 \; 0 \; 9.81 \frac{m}{s^2} \; 0 \,]^{\mathrm{T}}$.

The backward recursion to calculate force/torque vectors is carried according to the following relation

$$\mathbf{f}_i = {}^{i+1}_i\mathbf{X}^{\mathrm{T}}\, \mathbf{f}_{i+1} + \mathbf{f}_i^* \tag{7}$$

where $\mathbf{f}_i^*$ is the net force due to the ith body of the kinematic chain. The net force can be linearly parametrized as

$$\mathbf{f}_i^* = \mathbf{Y}(\dot{\mathbf{v}}_i, \mathbf{v}_i)\boldsymbol{\theta}_i \tag{8}$$

where $\mathbf{Y}$ is a regressor matrix and $\boldsymbol{\theta}_i$ is its corresponding parameter vector. See Appendix A for the derivation of the rigid-body regressor matrix and parameter vector.

B. Hydraulic actuator dynamics

The piston force of the cylinder equals to

$$f = p_1 A_1 - p_2 A_2 \tag{9}$$

where p_1 and p_2 denote chamber pressures, and A_1 and A_2 denote pressurized piston and bore areas. The time derivative of the piston force equals to

$$\dot{f} = \dot{p}_1 A_1 - \dot{p}_2 A_2 = \beta \left(\frac{Q_1 - A_1 \dot{x}}{x} - \frac{A_2 \dot{x} - Q_2}{S - x} \right) \tag{10}$$

where β is the effective bulk modulus, x is the piston displacement, and S is the maximum stroke of the piston. The valve-controlled volumetric flows Q_1 and Q_2 to the cylinder chambers can be written as

$$Q_1 = C_{\mathrm{PA}}\sqrt{p_S - p_1}\,\mathcal{S}(u)u + C_{\mathrm{AT}}\sqrt{p_1 - p_T}\,\mathcal{S}(-u)u \tag{11}$$

$$Q_2 = C_{\mathrm{PB}}\sqrt{p_S - p_2}\,\mathcal{S}(-u)u + C_{\mathrm{BT}}\sqrt{p_2 - p_T}\,\mathcal{S}(u)u \tag{12}$$

where u is the normalized valve control signal, p_S and p_T are the supply and return line pressures, C denotes the flow coefficients of each control edge (e.g., subscript PA denotes the orifice from supply line to chamber A, BT from second chamber B to tank, etc.), and $\mathcal{S}(\cdot)$ is a selective function defined as

$$\mathcal{S}(x) \triangleq \begin{cases} 1 & \text{if } x > 0 \\ 0 & \text{if } x \le 0 \end{cases} \tag{13}$$

Rearranging (10) and denoting the valve-controlled flow-related term with a scalar Q leads to the following expression

$$\underbrace{-\frac{Q_1}{x} - \frac{Q_2}{S - x}}_{Q} = \left(-\frac{A_1}{x} - \frac{A_2}{S - x} \right)\dot{x} - \frac{\dot{f}}{\beta} \tag{14}$$

Assuming the following relations $S > x > 0$ (i.e., the piston does not reach its end positions) and $p_S > p_1 > p_T \geqslant 0$ and $p_S > p_2 > p_T \geqslant 0$ always hold, the normalized valve control signal u corresponding to the flow-related scalar Q defined in (14) can be solved [6, p. 183] as

$$u = -\frac{\mathcal{S}(-Q)Q}{\frac{C_{\mathrm{PA}}\sqrt{p_S - p_1}}{x} + \frac{C_{\mathrm{BT}}\sqrt{p_2 - p_T}}{S - x}} \\ -\frac{\mathcal{S}(Q)Q}{\frac{C_{\mathrm{AT}}\sqrt{p_1 - p_T}}{x} + \frac{C_{\mathrm{PB}}\sqrt{p_S - p_2}}{S - x}} \tag{15}$$

The piston displacements x are mapped from measured encoder angles q with the following relation

$$x(q) = \sqrt{l_1 + l_2 - 2 l_1 l_2 \cos(q + q_0)} - x_0 \tag{16}$$

where l_1 and l_2 are distances from the cylinder pins to the joint axis connecting two rigid links (i.e., to the origin of the coordinates frames shown in Fig. 2), q_0 is a constant joint angle offset (i.e., the angle between the joint angle q and the angle formed between l_1 and l_2), and x_0 is a constant piston displacement offset. Differentiating the piston position x in (16) with respect to the joint angle q yields

$$\frac{\partial x}{\partial q} = \frac{l_1 l_2 \sin(q + q_0)}{\sqrt{l_1 + l_2 - 2 l_1 l_2 \cos(q + q_0)}} \tag{17}$$

which is the lever arm converting both joint velocities $\dot{q}$ into piston velocities $\dot{x}$ and piston forces f into joint torques τ.

III. PARAMETER IDENTIFICATION

A. Identification of rigid-body parameters

Not all of the standard inertial parameters appearing in the rigid-body parameter vector $\boldsymbol{\theta}$ are identifiable, because of restricted degrees-of-freedom and lack of full force/torque sensing [13–15]. Therefore, the dynamic model needs to be reduced to a form suitable for identification. More specifically, this model reduction consists of the following subtasks

(1) eliminating completely unidentifiable parameters, which have no effect on the measurable actuator torques, from the equations of motion

(2) regrouping partially unidentifiable (linearly dependent) parameters into identifiable linear combinations, so that unique parameter estimates can be acquired

The resulting vector of linearly independent coefficients $\boldsymbol{\theta}_\mathrm{b}$, also called the set of base inertial parameters, is a subspace of the complete rigid-body parameter vector. While it would be possible to reconstruct the full inertial parameter vector $\boldsymbol{\theta}$ from the experimentally identified coefficients $\boldsymbol{\theta}_\mathrm{b}$, this mapping from the dynamic coefficients to the full set of inertial parameters does not exist in general and is difficult to acquire [16]. Luckily, even though these identified coefficients lack intuitive physical meaning, they can be used to calculate the required actuator effort, which is sufficient for the purpose of robot control [15, p. 69].

Recently an analytical method to extract the identifiable coefficients appearing in the recursive N-E equations, named the Recursive Parameter Nullspace Algorithm (RPNA), was presented in [14]. RPNA only requires the kinematic parameters of the manipulator as its input, avoiding the drawbacks of traditional model reduction techniques, such as symbolic manipulation of the equations of motion based on parameter regrouping rules, or input-sensitive numerical analysis [13] (e.g., inspecting singular values of the regressor matrix). However, RPNA is only applicable to open-chain mechanisms, so the manipulator dynamics have to be simplified by not taking into account the dynamics of the closed chains formed by the cylinders and pistons. Hence, the effects of the cylinders and pistons will be lumped into the estimates of the link parameters. Identification of the closed chain dynamics would indeed be possible using symbolic regrouping techniques [17], but will be left for future work.
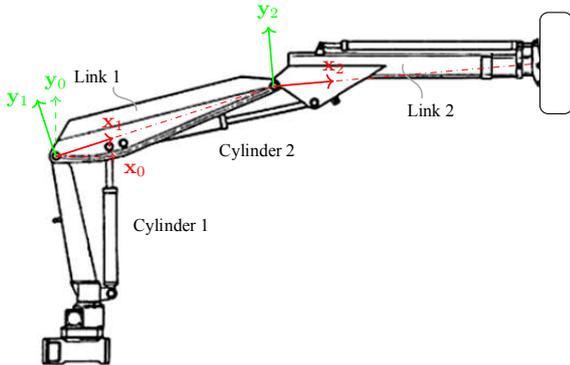

Fig. 2. Coordinate frame assignment for the manipulator.

Standard parameter	CAD value	Identified value
m_1	128,51 kg	*
c_{x1}	0,7404 m	*
c_{y1}	0,0368 m	*
I_{zz1}	95,97 kgm^2	*
m_2	641,42 kg	*
c_{x2}	1,7141 m	*
c_{y2}	0,0180 m	*
I_{zz2}	2074,71 kgm^2	*
Base parameter[1]	CAD value	Identified value
$mc_{x1} + m_2 a_1$	1121,4 kgm	1111,6 kgm
mc_{y1}	4,7 kgm	–117,3 kgm
$I_{zz1} + m_2 a_1^2$	1738,0 kgm^2	2305,2 kgm^2
mc_{x2}	1095,7 kgm	1074,2 kgm
mc_{y2}	92,0 kgm	–73,1 kgm
I_{zz2}	2074,7 kgm^2	2458,4 kgm^2
Friction coefficient	CAD value	Identified value
b_1	*	39872 Ns/m
b_2	*	77347 Ns/m

[1]Acquired using the *Recursive Parameter Nullspace Algorithm* [14].

While the piston seal friction of a hydraulic cylinder is a complex phenomenon, especially in the presliding regime (e.g., during motion reversal), for most applications a simple viscous friction model is a sufficient. Thus, a piston velocity-dependent viscous friction model was embedded to the rigid-body dynamic model without losing generality. The composite regressor matrix for the multi-rigid-body system can then be written as

$$\mathbf{Y} = \begin{bmatrix} \left[\mathbf{Y}(\dot{\mathbf{v}}_1, \mathbf{v}_1)\ \mathbf{s}_1(\frac{\partial x_1}{\partial q_1})^2\right] & \left[{}^2_1\mathbf{X}^\mathrm{T}\mathbf{Y}(\dot{\mathbf{v}}_2, \mathbf{v}_2)\ 0\right] \\ \mathbf{0} & \left[\mathbf{Y}(\dot{\mathbf{v}}_2, \mathbf{v}_2)\ \mathbf{s}_2(\frac{\partial x_2}{\partial q_2})^2\right] \end{bmatrix} \quad (18)$$

Before parameter identification, the rigid-body dynamics were reduced to a suitable form by removing the columns of $\mathbf{Y}$ corresponding to unidentifiable and redundant parameters, and the rows of $\mathbf{Y}$ and $\mathbf{f} = [\ \mathbf{f}_1\ \ \mathbf{f}_2\ ]^\mathrm{T}$ corresponding to unsensed force and/or torque components. After sampling and column stacking the reduced regressors $\mathbf{Y}_\mathrm{b}$ and regressands $\mathbf{f}_\mathrm{b}$, a least-squares estimate of the base inertial parameters was obtained as $\boldsymbol{\theta}_\mathrm{b} = (\mathbf{Y}_\mathrm{b}^\mathrm{T}\mathbf{Y}_\mathrm{b})^{-1}\mathbf{Y}_\mathrm{b}\ \mathbf{f}_\mathrm{b}$. Offline estimates of the time derivatives $\dot{q}$ and $\ddot{q}$ needed to recursively calculate the spatial velocities and accelerations were obtained by zero-phase low-pass filtering of encoder readings, followed by a central difference approximation. The low-pass filter was a second-order infinite-impulse response filter, with a damping ratio of 0.7 and a natural frequency of 5 Hz.

Force measurements were acquired indirectly via measuring cylinder chamber pressures to calculate piston forces using (9), before transforming the forces into equivalent torques affecting in the unactuated joints. The measured piston forces as well as the piston forces predicted using the identified parameters are shown in Fig. 3. The standard inertial parameters acquired by CAD modeling are provided in Table I, together with the identified base inertial parameters and friction coefficients. For comparison, base parameter values calculated from the CAD model parameters are also provided.
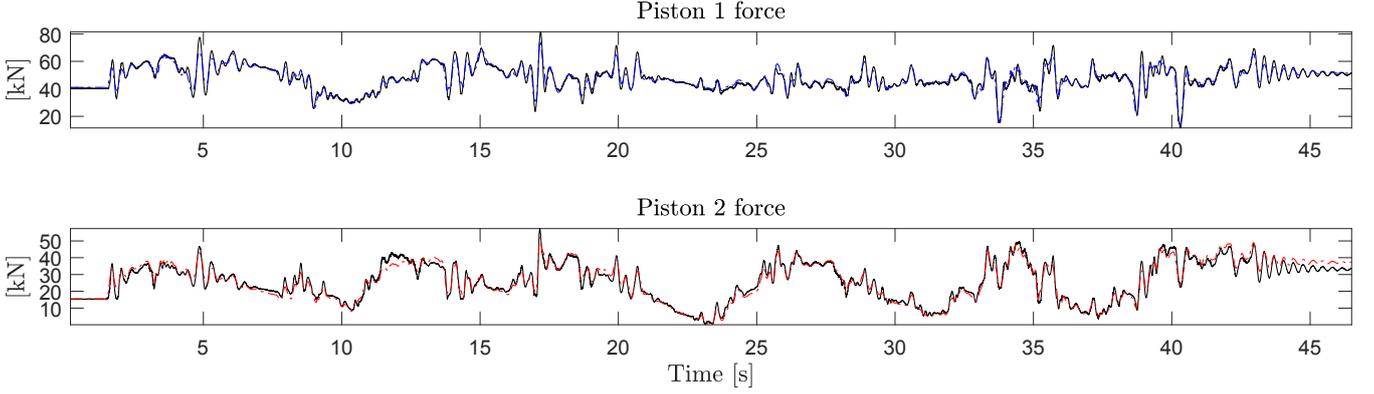
Fig. 3. Piston forces measured from chamber pressures (in *black*) and piston forces predicted using the identified rigid-body parameters (in *blue* and *red*).

B. Hydraulic parameters

We reuse the same actuator model parameters that were identified in our previous work [5]. The identified bulk moduli and valve flow coefficients are provided in Table II.

TABLE II
IDENTIFIED HYDRAULIC PARAMETER VALUES [5].

Parameter	Cylinder 1	Cylinder 2
$\beta^{-1}\left[\frac{\mathrm{N}}{\mathrm{m}^2}\right]$	$1,37 \cdot 10^{-9}$	$1,60 \cdot 10^{-9}$
$C_{\mathrm{PA}}\left[\frac{\mathrm{m}^3}{\mathrm{s}\sqrt{\mathrm{Pa}}}\right]$	$7,25 \cdot 10^{-7}$	$9,03 \cdot 10^{-7}$
$C_{\mathrm{AT}}\left[\frac{\mathrm{m}^3}{\mathrm{s}\sqrt{\mathrm{Pa}}}\right]$	$6,90 \cdot 10^{-7}$	$8,67 \cdot 10^{-7}$
$C_{\mathrm{PB}}\left[\frac{\mathrm{m}^3}{\mathrm{s}\sqrt{\mathrm{Pa}}}\right]$	$7,48 \cdot 10^{-7}$	$6,44 \cdot 10^{-7}$
$C_{\mathrm{BT}}\left[\frac{\mathrm{m}^3}{\mathrm{s}\sqrt{\mathrm{Pa}}}\right]$	$7,24 \cdot 10^{-7}$	$6,82 \cdot 10^{-7}$

The datasheet of Bosch Rexroth 4WRPEH10 servo valves states a 100 l/min flow rate at a 70 bar pressure difference (that is, 35 bar per control edge). The *normalized* valve flow coefficients equal to

$$C = \frac{Q}{\sqrt{\Delta p}} = \frac{\frac{100}{60000}\frac{m^3}{s}}{\sqrt{70 \cdot 10^5 Pa}} \approx 6,30 \times 10^{-7}\frac{m^3}{s\sqrt{Pa}}$$

IV. CONTROLLER STRUCTURE

This section will present the structure of the controller used in the experiments. Stability proofs for similar NMB control designs exist in [5–7]. Since the focus of this paper is in identification for control, the proof of stability is omitted due to limited space.

A. Control of the rigid-body subsystem

We begin by defining the required joint velocities as

$$\dot{\mathbf{q}}_{\mathrm{d}} = \mathbf{J}^{-1}\big(\dot{\mathbf{p}}_{\mathrm{d}} + k_p(\mathbf{p}_{\mathrm{d}} - \mathbf{p})\big) \tag{19}$$

where $\dot{\mathbf{p}}_{\mathrm{d}}$ is the desired Cartesian velocity of the end-effector, $\mathbf{p}_{\mathrm{d}}$ and $\mathbf{p}$ are measured Cartesian positions of the end-effector, and $\mathbf{J}$ is the manipulator Jacobian. The required joint velocities are transformed to required spatial velocities using (5).

Next, let us define the control law for the required spatial force to achieve the required spatial velocity. The required net force vector $\mathbf{f}_{id}^*$ is defined as

$$\mathbf{f}_{id}^* \triangleq \overbrace{\mathbf{Y}(\dot{\mathbf{v}}_{id}, \mathbf{v}_i)\boldsymbol{\theta}_{\mathrm{b}i}}^{\text{feedforward term}} + \overbrace{k_v(\mathbf{v}_{id} - \mathbf{v}_i)}^{\text{feedback term}} \tag{20}$$

Remark. The control approach in this paper differs from the methods in [6–10], where the required net force vector is defined as $\mathbf{f}_{\mathrm{d}}^* = \mathbf{M}\dot{\mathbf{v}}_{\mathrm{d}} + \mathbf{C}(\mathbf{v})\mathbf{v}_{\mathrm{d}}$. This modification allows us to use a standard 10-element rigid-body parameter vector, instead of the 13-element parameter vector given in [6, p. 386].

B. Control of the hydraulic subsystem

The required spatial velocity $\mathbf{v}_{id}$ and the required spatial force $\mathbf{f}_{id}$ are converted into a required piston velocity $\dot{x}_{id}$ and a required piston force f_{id} of the hydraulic actuator as

$$\dot{x}_{id} = \frac{\partial x_i}{\partial q_i}\dot{q}_{id} \tag{21}$$

$$f_{id} = \frac{\partial q_i}{\partial x_i}\big(\mathbf{s}_i^{\mathrm{T}}\mathbf{f}_{id}\big) + b_i\frac{\partial x_i}{\partial q_i}\dot{q}_i \tag{22}$$

The control law for the required flow-related term Q_{id} is defined as

$$Q_{id} \triangleq \overbrace{-\frac{A_1}{x_i} - \frac{A_2}{S - x_i} - \frac{\dot{f}_{id}}{\beta}}^{\text{feedforward term}}$$
$$\underbrace{-k_f(f_{id} - f_i) - k_x(\dot{x}_{id} - \dot{x}_i)}_{\text{feedback term}} \tag{23}$$

The required valve control signal u corresponding to the required flow-related term defined in (23) can be solved from by substituting Q in (15) by Q_{id}, which yields the following mapping into the normalized valve control signal

$$u_i = -\frac{\mathcal{S}(-Q_{id})Q_{id}}{\frac{C_{\mathrm{PA}}\sqrt{p_S - p_1}}{x_i} + \frac{C_{\mathrm{BT}}\sqrt{p_2 - p_T}}{S - x_i}}$$
$$-\frac{\mathcal{S}(Q_{id})Q_{id}}{\frac{C_{\mathrm{AT}}\sqrt{p_1 - p_T}}{x_i} + \frac{C_{\mathrm{PB}}\sqrt{p_S - p_2}}{S - x_i}} \tag{24}$$

V. EXPERIMENTS

The studied hydraulic manipulator is shown in Fig. 5. The hardware setup is the same as depicted in [7, 8], with the exceptions that the processor board is a dSPACE DS1005 and the controller sample time is 2 ms. To evaluate the controller performance, the same trajectory as in [5, 7] was employed. The path is a parallelogram with a height of 2 meters along the base Y-axis and a length of 1 meter along the X-axis. Motion profiles between the four corner points of the parallellogram
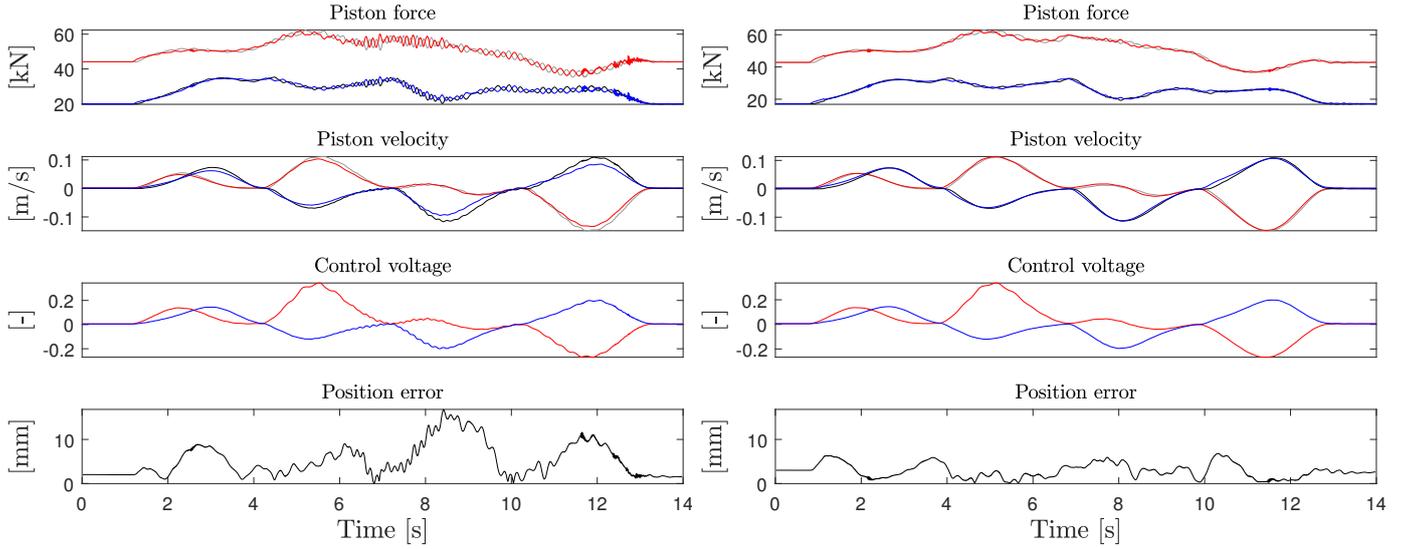
Fig. 4. Piston force tracking, piston velocity tracking, normalized control voltages and Cartesian position error *(i)* when using *nominal parameters* (left), and *(ii)* when using *identified parameters* (right). In the graphs illustrating force and velocity tracking, *red* and *grey* lines represent the measured and desired values for cylinder 1, while *blue* and *black* lines represent measured and desired values for cylinder 2, respectively.

were generated using quintic polynomials, with a transition time of 3 seconds between each point.

The feedback gains used in the experiments are provided in Table III. For real-time estimation of time derivatives, finite difference approximations were used, combined with an exponentially weighted moving-average filter to suppress noise. The filter is given by $y(n) = (1 - \alpha)y(n-1) + \alpha z(n)$, where the most recent input $z(n)$ is weighted by α and past values $y(n-1)$ are weighted by $(1 - \alpha)$. For both chamber pressure and joint encoder data, a value of $\alpha = 0.04$ was used.

TABLE III
FEEDBACK GAINS USED IN THE EXPERIMENTS.

Feedback gain	X-axis	Y-axis
$k_p[\frac{1}{s}]$	10	10
Feedback gain	Link 1	Link 2
$k_v[\frac{sN}{m}]$	3×10^4	3×10^4
$k_f[\frac{m}{sN}]$	1×10^{-8}	1×10^{-8}
$k_x[m]$	4×10^{-2}	4×10^{-2}

Force, velocity and position tracking, together with valve control signals, for the test using nominal parameters are provided in the left-hand side of Fig. 4, while the same data for the test when using identified parameters is provided on the right-hand side. Same feedback gains and filtering parameters were used in both cases. One can notice that the controller using the identified parameters performs significantly better, while the control signal is also better behaved. Meanwhile, the controller using the nominal parameters suffers from poor piston velocity tracking and noticeable ripple in piston force tracking.

As a summary, Table IV presents the values of several performance measures, namely the root mean square error (RMSE), maximum absolute position error $\max(|e|)$, and the normalized performance index ρ, which is the ratio of the maximum absolute error and the maximum recorded speed $\max(|v|)$. Using the nominal parameters leads to a maximum

position tracking error of more than 16 mm and a performance index value of $\rho = 0.0229$ (s), while using the identified parameters leads to a maximum position tracking error of less than 7 mm and a performance index value of $\rho = 0.0095$ (s).

The result achieved when using the identified parameters is a considerable improvement from the results reported in [5], where the tracking error was up to 16 mm and the performance index value was $\rho = 0.0231$ (s) when executing the same exact desired trajectory. When using ρ as a performance measure, the method proposed in this paper qualifies as second, right after the NMB controller presented in [7] ($\rho = 0.0050$ s), based on the state-of-the-art review made in [1].

TABLE IV
CONTROL PERFORMANCE BETWEEN CONSTANT PARAMETER CONTROL
WHEN USING IDENTIFIED PARAMETERS VERSUS NOMINAL PARAMETERS.

Hydraulic model	Rigid-body model	RMSE	$\max(|e|)$	$\frac{\max(|e|)}{\max(|v|)}$
Datasheet	CAD model[2]	6,5 mm	16,8 mm	0,0229 s
Identified	Identified	3,3 mm	6,8 mm	0,0095 s

[2]Identified viscous friction coefficients were used.

Fig. 5. The studied hydraulic manipulator.

VI. CONCLUSION

In this paper, a recursive N-E dynamics -based NMB control strategy with parameter identification was presented for a hydraulic manipulator. Base inertial parameters and frictional coefficients of the manipulator were identified from pressure transmitter and joint encoder data collected from the plant, in order to predict required actuator forces and required valve control signals. Experiments suggest that using the identified parameters leads to superior control performance, compared to using the nominal parameters acquired through CAD modeling and inspection of manufacturer datasheets.

In comparison to [5], the approach presented herein is more scalable in the sense that RPNA is applicable for serial manipulators with arbitrary kinematic topology. However, in the future, the identification procedure could be extended to account for the rigid-body dynamics of the cylinders and pistons, despite their relatively small contribution to the required actuator effort. This would require extending the model reduction techniques currently in use to cover the more complex dynamics of closed chains present in cylinder-actuated hydraulic manipulators.

Additionally, when extending the proposed method from planar motion to spatial 3D motion, physical consistency [18] of the estimated base inertial parameters should be ensured by using constrained optimization techniques instead of ordinary least-squares regression. Moreover, it remains to be studied whether augmenting the controller with parameter adaptation would significantly improve the force and/or position tracking performance, in comparison to constant parameter control.

REFERENCES

[1] J. Mattila, J. Koivumäki, D. G. Caldwell, and C. Semini, "A survey on control of hydraulic robotic manipulators with projection to future trends," *IEEE/ASME Trans. Mechatronics*, vol. 22, no. 2, pp. 669–680, 2017.

[2] S. Tafazoli, P. D. Lawrence, and S. E. Salcudean, "Identification of inertial and friction parameters for excavator arms," *IEEE Trans. on Robot. Autom.*, vol. 15, no. 5, pp. 966–971, Oct 1999.

[3] B. Li, J. Yan, G. Guo, H. Wang, and M. Zhang, "Identification of dynamic parameters and friction coefficients for a heavy-duty hydraulic manipulator," *Proc. the 10th World Congress on Intelligent Control and Automation*, pp. 3102–3106, July 2012.

[4] S. Sakai and Y. Maeshima, "A new method for parameter identification for N-DOF hydraulic robots," in *Proc. IEEE Int. Conf. on Robot. Autom. (ICRA)*, 2014, pp. 5983–5989.

[5] L. Hulttinen, J. Koivumäki, and J. Mattila, "Parameter identification for model-based control of hydraulically actuated open-chain manipulators," in *ASME/BATH Symp. on Fluid Power & Motion Control (FPMC)*, 2019.

[6] W.-H. Zhu, *Virtual Decomposition Control: Toward Hyper Degrees of Freedom Robots*. Springer, 2010.

[7] J. Koivumäki and J. Mattila, "High performance non-linear motion/force controller design for redundant hydraulic construction crane automation," *Automation in Construction*, vol. 51, pp. 59–77, 2015.

[8] ——, "Stability-guaranteed force-sensorless contact force/motion control of heavy-duty hydraulic manipulators," *IEEE Trans. Robot.*, vol. 31, no. 4, pp. 918–935, 2015.

[9] ——, "Stability-guaranteed impedance control of hydraulic robotic manipulators," *IEEE/ASME Trans. Mechatronics*, vol. 22, no. 2, pp. 601–612, 2017.

[10] J. Koivumäki, W.-H. Zhu, and J. Mattila, "Energy-efficient and high-precision control of hydraulic robots," *Control Engineering Practice*, vol. 85, pp. 176–193, 2019.

[11] R. Featherstone, *Rigid Body Dynamics Algorithms*. Springer, 2008.

[12] A. Müller, "Screw and lie group theory in multibody dynamics," *Multibody System Dynamics*, vol. 43, no. 1, pp. 37–70, May 2018.

[13] C. An, C. Atkeson, and J. Hollerbach, *Model-Based Control of a Robot Manipulator*. MIT Press, 1988.

[14] P. M. Wensing, G. Niemeyer, and J.-J. E. Slotine, "Observability in inertial parameter identification," May 2018. [Online]. Available: http://arxiv.org/abs/1711.03896v2

[15] K. Kozlowski, *Modelling and identification in robotics*. Springer, 1998.

[16] C. Gaz, F. Flacco, and A. De Luca, "Extracting feasible robot parameters from dynamic coefficients using nonlinear optimization methods," in *Proc. IEEE Int. Conf. on Robot. Autom. (ICRA)*, 2016, pp. 2075–2081.

[17] D. Surdilović, E. Lizama, and R. Lück, "Identification of dynamic parameters of large manipulator arms with closed kinematic loops," in *Robot Calibration*, R. Bernard and S. Albright, Eds., 1993, pp. 233–269.

[18] C. Sousa and R. Cortesão, "Physical feasibility of robot base inertial parameter identification: A linear matrix inequality approach," *Int. Journal of Robotics Research*, vol. 33, pp. 931–944, 2014.

[19] S. R. Ploen, "A skew-symmetric form of the recursive Newton-Euler algorithm for the control of multibody systems," in *Proc. American Control Conference*, vol. 6, 1999, pp. 3770–3773.

APPENDIX A
RIGID-BODY REGRESSOR AND PARAMETER VECTOR

The required net force vector in a body-fixed coordinate frame can be written as

$$\mathbf{f}_d^* = \mathbf{M}\dot{\mathbf{v}}_d + \mathbf{C}(\mathbf{v})\mathbf{v} \tag{25}$$

where $\mathbf{M}$ is the spatial inertia matrix [11, 14] and $\mathbf{C}(\mathbf{v})$ is a Coriolis-centrifugal matrix. The spatial inertia matrix for a single rigid body is composed as

$$\mathbf{M} = \begin{bmatrix} \mathbf{I} & [m\mathbf{c}\times] \\ -[m\mathbf{c}\times] & m\mathbf{1} \end{bmatrix} \tag{26}$$

where $\mathbf{I}$ is the inertia tensor of the body, defined as

$$\mathbf{I} = \begin{bmatrix} I_{xx} & I_{xy} & I_{xz} \\ I_{xy} & I_{yy} & I_{yz} \\ I_{xz} & I_{yz} & I_{zz} \end{bmatrix}$$

and m is the body mass and $\mathbf{c} = \begin{bmatrix} c_x & c_y & c_z \end{bmatrix}^{\mathrm{T}}$ is its center of mass location. A form of the Coriolis-centrifugal matrix $\mathbf{C}(\mathbf{v})$ suitable for control of multibody systems is derived in [19], and the resulting matrix is provided below.

$$\mathbf{C}(\mathbf{v}) = \begin{bmatrix} [\boldsymbol{\omega}\times]\mathbf{I} + \mathbf{I}[\boldsymbol{\omega}\times] & [m\mathbf{c}\times][\boldsymbol{\omega}\times] \\ -[\boldsymbol{\omega}\times][m\mathbf{c}\times] & m[\boldsymbol{\omega}\times] \end{bmatrix} \tag{27}$$

The net spatial force in (25) can be linearly parametrized with respect to the following standard vector of inertial parameters

$$\boldsymbol{\theta} = \begin{bmatrix} m & mc_x & mc_y & mc_z & I_{xx} & I_{xy} & I_{xz} & I_{yy} & I_{yz} & I_{zz} \end{bmatrix}^{\mathrm{T}} \tag{28}$$

The regressor matrix corresponding to the parameter vector $\boldsymbol{\theta}$ in (28) is expressed as follows

$$\mathbf{Y} = \begin{bmatrix} 0 & \dot{\boldsymbol{v}}_d + [\boldsymbol{\omega}\times]\boldsymbol{v} \\ -[(\dot{\boldsymbol{v}}_d + [\boldsymbol{\omega}\times]\boldsymbol{v})\times] & [\dot{\boldsymbol{\omega}}_d\times] + [\boldsymbol{\omega}\times][\boldsymbol{\omega}\times] \\ [\bullet\dot{\boldsymbol{\omega}}_d] + [\boldsymbol{\omega}\times][\bullet\boldsymbol{\omega}] & 0 \end{bmatrix}^{\mathrm{T}} \tag{29}$$

where the dot product operator $[\bullet(\cdot)]$ is defined as

$$[\bullet\boldsymbol{\omega}] = \begin{bmatrix} \omega_x & \omega_y & \omega_z & 0 & 0 & 0 \\ 0 & \omega_x & 0 & \omega_y & \omega_z & 0 \\ 0 & 0 & \omega_x & 0 & \omega_y & \omega_z \end{bmatrix}$$

The regressor matrix used for parameter identification is acquired by replacing the desired values in (29) by measured values. The regressor matrix then corresponds to the one given in [13, p. 71], except for the terms where linear acceleration appears. This is due to a differing definition of acceleration in the boxy-fixed [6, 11] and hybrid [13] formulations of the recursive N-E algorithm; see [12] for a thorough comparison of different representations of rigid-body dynamics.